LA-UR-81-987

CONF-810509--27

MASTER

TITLE: A ONE-DIMENSIONAL MODEL OF THE DYNAMIC LAYER BEHAVIOR IN A SALT-GRADIENT SOLAR POND

AUTHOR(S): Kenneth A. Meyer

SUBMITTED TO: Solar Rising Conference and Exposition
Philadelphia Civic Center
May 26-30, 1981



University of California

LOS ALAMOS SCIENTIFIC LABORATORY
Post Office Box 1663 Los Alamos, New Mexico 87545
An Affirmative Action/Equal Opportunity Employer

Form No. 836 R3
St. No. 2629
12/78

UNITED STATES
DEPARTMENT OF ENERGY
CONTRACT W-7405-ENG. 36

# A ONE-DIMENSIONAL MODEL OF THE DYNAMIC LAYER BEHAVIOR IN A SALT GRADIENT SOLAR POND*

Kenneth A. Meyer
Los Alamos National Laboratory
P.O. Box 1663, MS/571
Los Alamos, NM 87545

## ABSTRACT

A numerical model has been developed to describe the time-dependent behavior of the interfaces between the convecting and nonconvecting regions of a salt gradient solar pond. Salinity and temperature profiles, as functions of time, are also determined by the model. The model utilizes empirical correlations from the oceanographic literature that describe the heat and salt fluxes across the interfaces. We find agreement of the calculated behavior with observations made on laboratory-scale solar pond simulation experiments.

## 1. INTRODUCTION

Salt gradient solar ponds are large-area, low-cost devices for the collection and storage of solar energy. Typically, a pond consists of three fluid regions: an upper convecting region of uniform, relatively low salinity and temperature; a stagnant insulating gradient region where salinity and temperature increase with depth; and a lower convecting thermal storage region of uniformly high salinity and temperature. Sunlight penetrating the pond warms the bottom region of water. Heat loss is minimized because of the insulation provided by the nonconvecting region.

The effectiveness of a solar pond is determined, to a large extent, by the thickness of the various regions. The upper convecting region absorbs radiation but provides no insulation; therefore, it is desirable to minimize its thickness. The gradient region provides the pond's insulation, and its reduction below optimum design thickness will result in increased heat loss. The thickness of the lower convecting region determines the amount of thermal storage available.

In operating ponds, unplanned growth of the upper convective region has been observed, as well as upward migration of the lower boundary of the gradient region. These motions occur even though the gradient region itself is hydrodynamically stable. The purpose of the numerical model described in this paper is to predict the motion of these regions so as to facilitate pond design and operation.

## 2. BACKGROUND

A review of the literature indicates that the oceanographic community has done extensive work in the area of thermohaline systems that is applicable to salt gradient ponds.

As compared to the three-region solar pond, the system extensively studied by the oceanographers consists of two convecting regions separated by a diffusive interface. The lower region is hotter, saltier, and more dense than the upper. The interface varies in thickness from a few millimeters to approximately 5 cm. The thicker interfaces exhibit a nonconvecting diffusive core, separated from the convecting regions by layers of intermittent turbulent fluctuations. Researchers have obtained empirical relations for the salt and heat fluxes across a diffusive interface as a function of the temperature and salinity steps across the interface.

Workers at Purdue University (Ref. 1) attempted to simulate solar ponds in laboratory tanks. They established quasi-static systems in which the convecting regions were separated by 25 to 65 cm of diffusive core. Shadowgraphs indicate boundary layer formation between the diffusive core and the convecting regions.

We suspect that very similar boundary layer behavior exists in ponds. The boundary layers above and below a gradient region

*This work was supported in part by the US Department of Energy, Offices of Solar Applications for Buildings and Solar Applications for Industry.

may be two halves of the interface layer that occurs at the temperature and salinity step of interest to oceanographers. Furthermore, we speculate that the flux relation obtained across the relatively thin diffusive interface of the oceanographic studies also applies across the boundary layers separating the convecting regions from the gradient region in solar ponds. We find that the applicability of this flux relation to solar ponds is partially supported by data taken in the Ohio State University salt gradient pond.

Most of the oceanographic layer experiments and the solar pond simulations have been considered as quasi-static; that is, the interface positions tend to move slowly with time. We are testing the hypothesis that boundary layer motion occurs when the salt and heat fluxes cause a violation of either static stability (density increasing downward) across the layer or dynamic stability (an infinitesimal oscillatory instability) in the gradient adjacent to the boundary layer.

We have developed a one-dimensional model of the solar pond using the diffusion equation to describe the salt and heat transport. Molecular diffusivities are used in the nonconvecting region, eddy diffusivities in the convecting region, and the aforementioned flux relation is used to connect regions. A microscopic description of the boundary layer is not attempted. Transition from nonconvecting to convecting status is based on the static and dynamic stability relations. Our calculations show good agreement with data from pond simulation experiments at Purdue.

## 3. NUMERICAL MODELING

The pond configuration assumed in the one-dimensional numerical model is a three-region system with boundary layers separating the convecting regions from the nonconvecting regions. The time-dependent diffusion equation is used to determine both the heat and salt fluxes. The temperature distribution in the pond is obtained from

$$\rho C_p \frac{\partial T}{\partial t} = \frac{\partial}{\partial x}\left(k_T \frac{\partial T}{\partial x}\right) + q(x,t) - L(x,t) \quad . \quad (1)$$

In the nonconvecting region, the molecular conductivity is used for $k_T$; in the convecting regions, an eddy conductivity is used. The upper boundary conditions allow for convection, conduction, evaporation, and radiation at the surface. The lower boundary of the fluid is coupled to the ground, or an insulated boundary can be assumed.

The salinity profile is determined from

$$\frac{\partial \rho_s}{\partial t} = \frac{\partial}{\partial x}\left(D_s \frac{\partial \rho_s}{\partial x} + D_{ST} \frac{\partial T}{\partial x}\right) \quad . \quad (2)$$

The second term on the right side of Eq. 2 is the Soret term, and it represents the transport of salt induced by the temperature gradient. It stems from an irreversible thermodynamic approach to the diffusion process. In the nonconvecting region, the molecular diffusivity is used, whereas an eddy diffusivity is used in the convecting region. The upper and lower fluid surfaces are considered impermeable to salt.

The nonconvecting region must satisfy the dynamic stability criterion associated with a double diffusive (salt and heat) system. This stability condition requires that the gradient region satisfies

$$(\nu + D_T)\alpha \frac{\partial T}{\partial x} + (\nu + D_s)\beta \frac{\partial \rho_s}{\partial x} \geq 0 \quad , \quad (3)$$

where x is position downward from the surface. If Eq. 3 is not satisfied in a portion of the nonconvecting region, that portion is flagged as convecting, and the appropriate eddy diffusivities are used.

A further stability requirement is that static stability (density increasing downward)

$$\frac{\Delta \rho}{\Delta x} = \alpha \frac{\Delta T}{\Delta x} + \beta \frac{\Delta \rho_s}{\Delta x} \geq 0 \quad , \quad (4)$$

is satisfied across the boundary between a convecting and nonconvecting region. If it is not satisifed, the convecting region is allowed to encroach on the nonconvecting one.

The interface conditions that are applied between convecting and nonconvecting regions are taken from oceanographic thermohaline studies and are described below.

The heat flux across a double diffusive interface can be expressed as (Ref. 2)

$$H = (0.0086)\, k_T\, (g\alpha/D_T\nu)^{1/3}\, \Delta T^{4/3} \cdot \exp\left|4.6 \exp\left[-0.54(R - 1.0)\right]\right| \quad . \quad (5a)$$

For ease in computation, when applying this across the boundary layer, we express the heat flux as an effective thermal conductivity,

$$\hat{k}_T = (0.0086)\,\Delta x\, k_T\,(g\alpha\Delta T/\nu D_T)^{1/3} \cdot \exp\left\{4.6 \exp\left[-0.54(R - 1.0)\right]\right\} \quad , \tag{5b}$$

where $\Delta x$, the mesh spacing, appears because the boundary layer is assumed to be one computational zone thick.

This correlation was obtained using the temperature difference, $\Delta T$, and the buoyancy ratio, R, existing across the entire diffusive interface; hence, there is no a priori reason to believe that it should also apply across the boundary layer. Fortunately, in the solar pond most of the thermal resistance is across the gradient region, and this determines the heat flux. In a quasi-static situation, therefore, the boundary layer heat flux will essentially be imposed by the controlling gradient region. Calculated results were insensitive to the choice of boundary layer thermal conductivity over a wide range of conductivities. We are currently using the greater of Eq. 5b and the molecular conductivity as the effective boundary layer conductivity.

The oceanographic results suggest that the salt flux across a diffusive interface is related to the heat flux by expressions of the form,

$$\frac{\rho C_p \beta F_s}{\alpha H} = (2.0 - C) - (1.0 - C)R \quad , \tag{6a}$$

$$1 \le R \le 2 \quad ,$$

and

$$\frac{\rho C_p \beta F_s}{\alpha H} = C, \quad R > 2.0 \quad . \tag{6b}$$

While the correlation for the heat flux (Eq. 5a) across a double diffusive interface is probably not directly applicable across the boundary layer, we postulate that the associated empirical salt flux to heat flux correlation (Eqs. 6a and 6b) across a diffusive interface does apply across the boundary layer. In particular, we feel that this correlation applies to solar pond boundary layers, provided one restricts consideration to the expression for $R > 2$. We believe that the salt flux to heat flux correlation applies across the boundary layer because in a quasi-static system, the flux ratio that holds across the entire diffusive interface must hold equally well across each of the boundary layers and across the diffusive core. If this were not so, the assumed quasi-static condition would be violated.

The left sides of Eqs. 6a and 6b are in the form of a dimensionless flux ratio. Early investigation indicated that C, a measured quantity, was a constant and equal to 0.15. Current speculation is that the flow regime described by Eq. 6a has turbulent bursts that convect fluid across the interface, while at the high stability ratio ($R > 2$) described by Eq. 6b, the interface possesses a diffusive core across which no convection occurs.

Later investigations (Ref. 2) indicate that C is not a constant, but a function of the heat flux. Figure 1 shows the range of C as a function of heat flux as measured by Marmorino and Caldwell in layered systems. In these systems the total interface thickness ranged from 1 to 4 cm, much thinner than the gradient region thickness for a solar pond (40 to 100 cm). Nielsen (Ref. 3) has published data on measurements that he took in the gradient region of a solar pond. These data were taken near the boundaries between the gradient and the convective regions. We have expressed Nielsen's findings in a form compatible with the Marmorino and Caldwell results and plotted them as the solid curve on Fig. 1. We believe that the relatively good agreement supports our conjecture that the same physical phenomena are present in both the layered thermohaline systems and salt gradient ponds.

Again, for ease in computation, we define an effective boundary layer salt diffusivity, $\hat{D}_s$, as

$$\hat{D}_s = \frac{\hat{k}_T}{\rho C_p R}\left[(2.0 - C) - (1.0 - C)R\right] \quad , \tag{6c}$$

$$1 \le R \le 2 \quad ,$$

and

$$\hat{D}_s = \frac{\hat{k}_T}{\rho C_p R} C \quad , \quad R > 2.0 \quad . \tag{6d}$$

The system of equations (1-6) was replaced by its finite difference analog and solved using an implicit procedure.

## 4. COMPARISON WITH EXPERIMENT

Our first calculation was an attempt to reproduce the experimental results obtained by Purdue University investigators (Ref. 1)

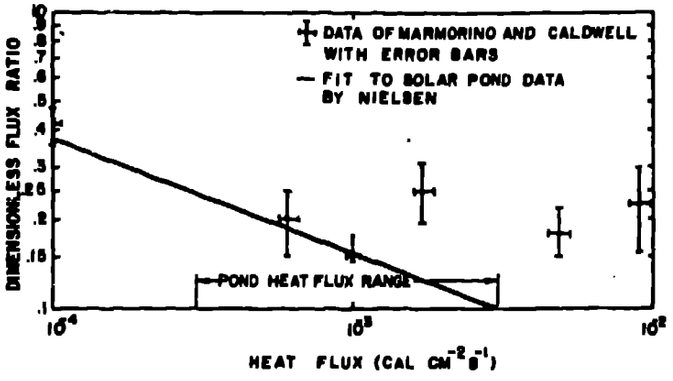


Fig. 1.
Experimentally measured values of the dimensionless salt to heat flux ratio, C, vs heat flux for R > 2.

in a bottom-heated solar pond simulation experiment. The experimental tank was filled with 68 cm of solution having an initial temperature of 24°C and a linear salinity profile varying from 25% by weight NaCl at the bottom to 0 at the top. The gradient region thickness varied from 65 to 25 cm during the course of the experiment.

The experimental tank was not well insulated; hence, adjustments had to be made in the numerical heating rate in order to match the experiment. The numerical heating rate appears reasonable when compared to that inferred from measured temperature profiles through the gradient region. The mode of heating was first a gradual increase in heat input from the first day through the ninth day. From Day 9 through Day 30 the heating rate was held constant. During the steady heating phase, the experimental heater output was 244 W/m$^2$. The rate inferred from the measured temperature gradient is about 65 W/m$^2$; therefore, the calculation assumed 65 W/m$^2$. The free surface heat loss coefficient was adjusted to give a top layer temperature near the measured value.

Figures 2 and 3 compare our calculation with experimental data. Overall, the agreement is quite good. Figure 2 indicates that the model reproduces the region boundary motions very well during the time the convection regions are advancing into the gradient region. Calculated temperature histories of the convecting regions are compared with experiment in Fig. 3; again, agreement is good.

## 5. CONCLUSIONS

The calculations described in the preceding paragraph support our conjecture that the interface flux relation of Eq. 6b is valid for solar ponds since the gradient layer thickness in the Purdue experiments (25 to 65 cm) was more akin to that in ponds than to that of oceanographic layer experiments (1 to 4 cm). These calculations are not conclusive, however, because of the crude nature of Purdue thermal data and the lack of detailed salinity data.

The agreement with the experiment does indicate that our numerical model shows promise as a potential design tool for solar ponds.

It is possible to make a plausible physical interpretation, based on the boundary layer flux relation (Eq. 6b), as to the cause of the motion of region boundaries in a solar pond. In a pond, the heat flux is determined by the temperature drop across the gradient region. This heat flux also occurs in the boundary layer. The boundary layer salt flux is determined by the boundary layer heat flux in accordance with Eq. 6b. If, at the lower convecting region/gradient region boundary, this salt flux is greater than that permitted by diffusion in the gradient region, there will be a tendency for salt to build up in the gradient region adjacent to the boundary layer. Eventually this salt buildup (and related density increase) will result in a loss of static stability across the boundary layer and subsequent advancement of the convecting region. This interpretation implies that in salt gradient ponds there is a maximum permissible heat flux above which gradient control will be needed.

## 6. NOMENCLATURE

| | |
|---|---|
| $C_p$ | Specific heat (J/g°C) |
| $D_s$ | Salt diffusivity (cm$^2$/s) |
| $D_{ST}$ | Soret coefficient (g/cm$^2$s°C) |
| $D_T$ | Thermal diffusivity (cm$^2$/s) |
| $R_s$ | Effective boundary layer diffusivity (cm$^2$/s) |
| $F_s$ | Salt flux (g/cm$^2$ s) |
| g | Gravitational acceleration (cm/s$^2$) |
| H | Heat flux (W/cm$^2$) |
| $k_T$ | Thermal conductivity (W/cm°C) |
| $k_T$ | Effective boundary layer conductivity (W/cm°C) |

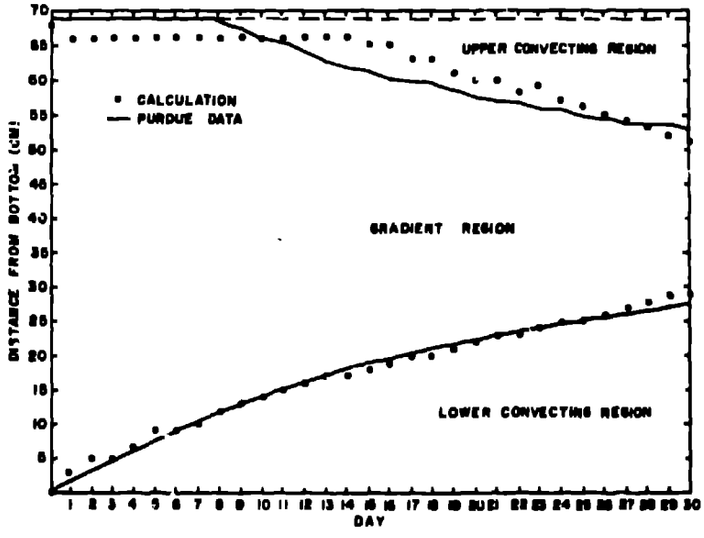


Fig. 2.
Region boundary positions vs time during the heating phase.

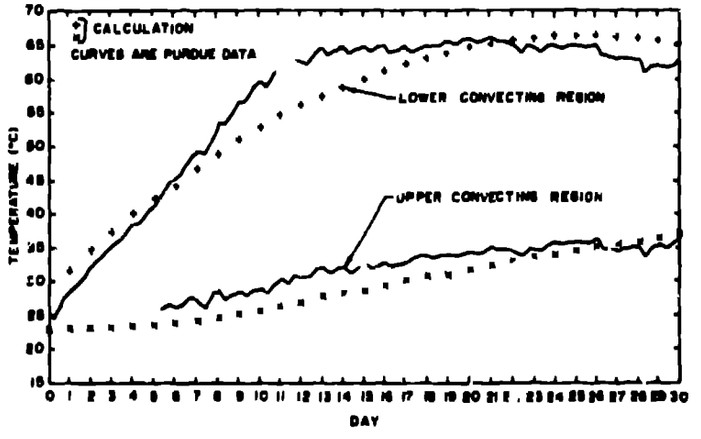


Fig. 3.
Convecting region temperatures vs time during the heating phase.

| | |
|---|---|
| L | Energy removed at depth x ($W/cm^3$) |
| q | Solar energy absorbed at depth x ($W/cm^3$) |
| R | $R = B\Delta\rho_s/\alpha\Delta T$ |
| T | Temperature (°C) |
| x | Vertical distance (cm) |
| $\alpha$ | Thermal coefficient of expansion (1/°C) |
| $\beta$ | Salinity expansion coefficient ($cm^3/g$) |
| $\nu$ | Kinematic viscosity ($cm^2/s$) |
| $\rho$ | Density ($g/cm^3$) |
| $\rho_s$ | Solute density ($g/cm^3$) |

## 7. REFERENCES


1. C. J. Poplawsky, "Laboratory Simulation of the Solar Pond, Double-Diffusive, Thermohaline Systems," Purdue University Masters Thesis, December 1980.

2. G. O. Marmorino and D. R. Caldwell, "Heat and Salt Transport Through a Diffusive Thermohaline Interface," Deep Sea Research, 23, 59 (1976).

3. C. E. Nielsen, "Control of Gradient Zone Boundaries," Proceedings of the International Solar Energy Society Meeting, Atlanta, Georgia, May 28, 1979.